

Model Predictive Control for Low Pressure Exhaust Gas Recirculation with Scavenging

Ashley P. Wiese, Anna G. Stefanopoulou, Amey Y. Karnik, Julia H. Buckland

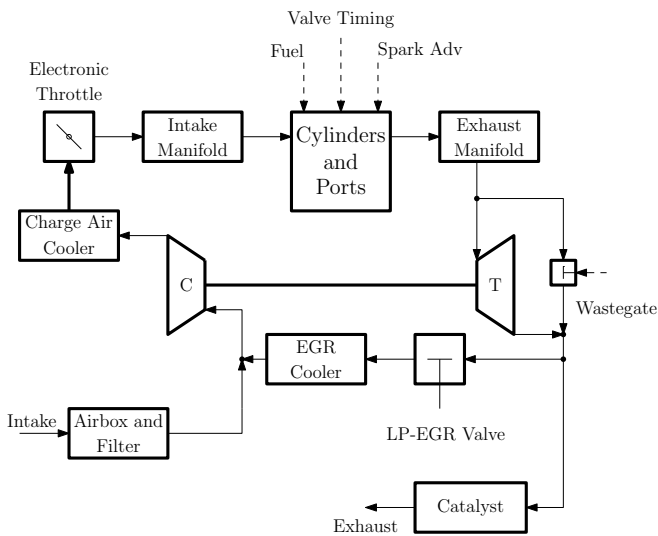


Figure 1. Turbocharged gasoline engine with LP-EGR

Abstract—Low-Pressure Exhaust Gas Recirculation (LP-EGR) has been shown to be an effective means of improving fuel economy and suppressing knock in downsized, boosted, spark ignition engines. However, the transport delays inherent in LP-EGR systems can lead to combustion instability and misfire during tip-out events.

This paper implements a Linear Time-Varying (LTV) Model Predictive Control (MPC) to track transient demand in LP-EGR rates, while limiting EGR in the intake manifold at lower loads. The LTV-MPC leverages high overlap causing short-circuit flow behaviour through the cylinders that may improve EGR evacuation rates.

The controller is tested in simulation for representative tip-out transients. The amount of torque demand preview required to satisfy the constraint on intake manifold burned gas is investigated, and the benefit of including high overlap valve timing is assessed.

I. INTRODUCTION

Cooled, external Exhaust Gas Recirculation (EGR) can be effective for improving fuel economy and for suppressing knock in turbocharged, spark ignition engines [11]. Low Pressure EGR (LP-EGR) is an approach for delivering external EGR, where exhaust gas is extracted downstream of the turbine and reintroduced upstream of the compressor (e.g. Fig. 1).

Despite the known benefits of LP-EGR [1], [11], [12], [8], its use is limited by transport delays in the air path between the LP-EGR valve and the intake manifold. These delays

Table I
 LP-EGR EVACUATION IMPROVEMENT [13]

Engine Speed (rpm)	$BMEP$ (bar)	Initial LP-EGR (%)	Reduction in EGR evacuation time due to valve overlap
2000	14.1	15	15%
2000	15.9	10	24%

slow the response time in changing the EGR concentration in the intake manifold. This is of particular concern during a reduction in engine torque demand, or ‘tip-out event’ as slow LP-EGR response may delay the reduction of EGR concentration despite closing the EGR valve. The resulting combination of high EGR at low load is problematic due to lower external EGR tolerance at low load conditions that leads to unacceptably slow combustion rates. This effectively constrains the maximum LP-EGR rate that can be sustained at high load prior to a tip-out.

In a preceding work [13], a simulation study was undertaken examining evacuation rates of LP-EGR, and the potential benefits of using high valve overlap, thereby inducing short-circuit (scavenging) flow [6] to reduce EGR evacuation times by up to 25% compared with baseline valve timing. [13] focused on a constant torque preview period, prior to tip-out, and showed that reductions in evacuation times could be achieved by introducing high valve overlap, and subsequently short-circuit flow, during the preview period (c.f. Table I). This result has motivated an extension of [13] to transient control of LP-EGR and VVT during a tip-out event.

This paper seeks to address the transient EGR control problem using a Model Predictive Control (MPC) approach. Within this framework, a simple constraint on intake manifold burned gas concentration ξ_i is adopted, as shown in Fig. 2. The operating range is divided into high, and low-load regimes separated by a threshold Brake Mean Effective Pressure $BMEP_{thr}$. While operating above $BMEP_{thr}$, ξ_i is constrained by the target external EGR rate, while below $BMEP_{thr}$, a single, conservative, upper bound $\xi_{i,thr}$ ($BMEP_{thr}$) is prescribed.

In practice, the constraint on intake manifold burned gas concentration ξ_i is complex, influenced by the cylinder geometry, engine operating condition, and combustion behaviour. Furthermore, although $BMEP_{thr}$, $\xi_{i,thr}$ pairings are expected to be a function of engine speed, this paper focuses on constant speed operation, and this dependence is not implemented.

Above $BMEP_{thr}$, (and at low engine speeds) it is desirable to maintain higher levels of external EGR, measured upstream

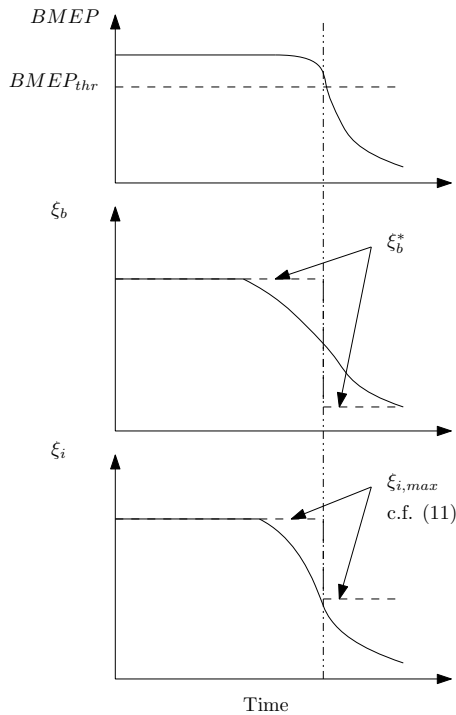


Figure 2. Tip-out Evacuation Problem

of the throttle (denoted as ξ_b^*). Prior to, or during a tip-out, ξ_i must be reduced to the threshold value before reaching $BMEP_{thr}$. Given the delays inherent in LP-EGR systems, this may require preview information. With connected and autonomous vehicles, a short preview period may be available. One aim of this paper is to systematically quantify the preview required to satisfy the burned gas concentration constraint. A good control approach for such an investigation is MPC, as it allows this preview period to be incorporated, while inherently managing the constraints on burned gas concentration.

MPC has been previously applied to the air path of gasoline engines for idle speed control [2], [10], boost control [9], and transient torque tracking [3]. However, these studies do not include external EGR. Transient control of external EGR systems appears to have received more attention on diesel engines [7], [14], [5], [15]. While these studies commonly focus on high-pressure (HP)-EGR (e.g. [7]), dual-loop [14], [5] and LP-EGR [15] systems have also been considered. As diesel engine EGR primarily affects emissions rather than torque, the tip-out constraint on burned gas concentration is less restrictive than for gasoline engines. Additionally, of the preceding studies, only [3] appears to explicitly consider high valve overlap, as a potential means of improving transient torque response.

This paper presents a simulation study of a Linear Time-Varying Model Predictive Control (LTV-MPC) approach, specifically for managing the LP-EGR loop for a gasoline, turbocharged, direct injection (GTDI) engine, with dual-independent VVT. An LTV approach is employed, as the

model characteristics are expected to change substantially with $BMEP$ and VVT variation. The developed MPC is responsible for the LP-EGR valve, and has the authority to modify VVT from an existing, baseline calibration. The MPC assumes a torque control strategy already exists to manage throttle, wastegate, fuel and spark timing.

The simulation test-bed for the controller is a 2-state nonlinear model of the external EGR loop of the GTDI engine. This model, described in Section II, is a reduced order form of a higher-order, mean value engine model (MVEM [4]), and represents the burned gas concentration dynamics in the intake manifold and the volume between the compressor and throttle. The predictive component of the MPC is obtained by linearising the 2-state model at the beginning of each MPC calculation. This linearisation can be performed analytically, which limits the computational expense.

The resulting LTV-MPC is applied to a series of engine tip-out/EGR evacuation scenarios, and the impact of various cost function weights is discussed. Finally, the tuned LTV-MPC is used to evaluate the torque preview requirements, with and without high valve overlap, to determine what benefit VVT and preview may provide for EGR evacuation rates during constant speed load transients.

II. NONLINEAR MODEL

In this section, a 2-state, nonlinear model is developed to act as a test-bed for controller simulations. Additionally, this model is linearised to act as the predictive component of a Linear, Time-Varying (LTV) MPC. The model is based on data from a GT-Power model of the same engine, and is subject to the following simplifying assumptions:

Assumption 1. A separate, open-loop torque control exists that takes the current torque demand $BMEP^*$, engine speed N_{eng} , intake and exhaust valve timings ζ_i, ζ_e , and the intake manifold burned gas concentration ξ_i , and outputs a throttle angle θ , to achieve the torque demand.

$$\theta = \Theta(N_{eng}, BMEP^*, \zeta_i, \zeta_e, \xi_i) \quad (1)$$

Assumption 2. The pressure and flow rate dynamics are assumed to be instantaneous relative to the burned gas concentration the intake manifold and pre-throttle ξ_b volume. The intake manifold pressure P_i , is set by the torque controller, while the wastegate is used to track a reference value of pre-throttle pressure P_b ,

$$P_i = \mathcal{P}_i(N_{eng}, BMEP^*, \zeta_i, \zeta_e, \xi_i), \quad (2)$$

$$P_b = \mathcal{P}_b(N_{eng}, BMEP^*). \quad (3)$$

The flow rate through the gas path W_{eng} is then set by a steady-orifice equation, representing the throttle

$$W_{eng} = W_{th} = \mathcal{W}_{th}(P_i, P_b, \theta). \quad (4)$$

While the boost pressure dynamics are typically slower than the intake manifold pressure and engine flow dynamics, it is assumed that they are still fast relative to the concentration dynamics.

Remark 1. This assumption was tested in simulation, comparing the output of the resulting differential-algebraic model with simulation traces from a higher-fidelity GT-Power model of the same engine. These results showed reasonable agreement (within 0.005 of fractional EGR concentration).

Assumption 3. The change in intake manifold and pre-throttle gas temperatures T_i , T_b are sufficiently small, or slow, that they may be treated as constant. Furthermore, the gas constant for mixtures of fresh air and burned gas may be reasonably approximated by R_{air}

Remark 2. This isothermal assumption is a common simplification in MVEM [4]. Variations in temperature and gas constant due to external EGR may occur, but these are expected to be small given an effective intercooler, and the relative similarity between the air and exhaust gas constants

Assumption 4. The response time of the LP-EGR flow rate into the compressor W_{LP-EGR} is fast enough that it may be treated as instantaneous. Consequently, W_{LP-EGR} is treated as an input to the system that the MPC has direct authority over. Furthermore the movement of the throttle and VVT is assumed to be instantaneous relative to the burned gas concentrations.

Given these assumptions, a two-state, lumped parameter model of the intake manifold and pre-throttle burned gas concentrations may be defined as¹

$$\dot{\xi}_b = \frac{R_{air}T_b}{V_bP_b} (W_{LP-EGR} - W_{eng}(\zeta_i, \zeta_e, BMEP^*, N_{eng}, \xi_i) \xi_b), \quad (5)$$

$$\dot{\xi}_i = \frac{R_{air}T_i W_{eng}(\zeta_i, \zeta_e, BMEP^*, N_{eng}, \xi_i)}{V_i P_i} (\xi_b - \xi_i), \quad (6)$$

Or, henceforth expressed in vector form:

$$\dot{\mathbf{x}} = \mathbf{f}(\mathbf{x}, \mathbf{u}, \mathbf{v}), \quad (7)$$

where

$$\mathbf{x} = [\xi_b, \xi_i]^T, \quad \mathbf{u} = [\zeta_i, \zeta_e, W_{LP-EGR}]^T$$

$$\mathbf{v} = [BMEP^*, N_{eng}]^T$$

A. Linear, Time-Varying Predictive Model

While (7) provides acceptable agreement with the corresponding GT-Power simulation model, the nonlinearity with respect to \mathbf{u} substantially increases the computational effort required for practical implementation of MPC. It is therefore proposed to use a linear, time-varying model for the predictive component of an MPC. At each time instant t_j , (7) is linearised around the current states and exogenous inputs, and the previous control input, denoted as \mathbf{x}_j , \mathbf{v}_j and \mathbf{u}_{j-1} respectively, to provide a continuous state-space model

$$\Delta \dot{\mathbf{x}}_k = \mathbf{A}(t_j) \Delta \mathbf{x}_k + \mathbf{B}_{opt}(t_j) \Delta \mathbf{u}_k + \mathbf{B}_{exo}(t_j) \Delta \mathbf{v}_k + \mathbf{f}(\mathbf{x}_j, \mathbf{u}_{j-1}, \mathbf{v}_j), \quad (8)$$

¹Note, that while W_{eng} is more commonly a function of ξ_i, ξ_e and P_i , the dependence on P_i is replaced with (2), according to Assumption 2.

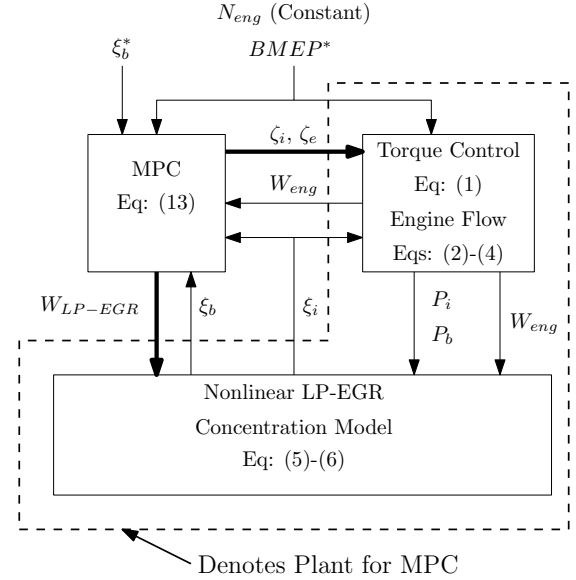


Figure 3. Simulation and Control Block Diagram

where the term $\mathbf{f}(\mathbf{x}_j, \mathbf{u}_{j-1}, \mathbf{v}_j)$ is a necessary part of the linearisation when $\mathbf{x}_j, \mathbf{u}_{j-1}, \mathbf{v}_j$ is not an equilibrium point of the system. Assuming that both control \mathbf{u} , and exogenous \mathbf{v} inputs are piecewise constant for a given sample period t_s , the discrete equivalent of (8) is

$$\Delta \mathbf{x}_{k+1} = e^{\mathbf{A}(t_j)t_s} \Delta \mathbf{x}_k + \int_0^{t_s} e^{\mathbf{A}(t_j)(t_s-\tau)} d\tau \mathbf{B}(t_j) \times [\Delta \mathbf{u}_k + \Delta \mathbf{v}_k + \mathbf{f}(\mathbf{x}_j, \mathbf{u}_{j-1}, \mathbf{v}_j)]. \quad (9)$$

The state trajectories of both (7) and (9) were compared for a common set of representative inputs. For the inputs considered, and using a sample time of 0.1 s, the concentrations reported by (9) were shown to be within 1% point of the concentrations reported by (7), for prediction horizons $t_p \leq 0.8$ s. Therefore, the prediction horizon of the following LTV-MPC will be limited to this value. A formal stability analysis is beyond the scope of this paper. Nevertheless, the prediction horizons implemented in the following sections do not result in unstable behaviour during representative simulations.

III. MPC - PROBLEM FORMULATION

In the following section, an LTV-MPC is developed for a gasoline LP-EGR circuit. The controller is developed in simulation, using the nonlinear model (5)-(6), and the engine flow model (2)-(4), to represent the plant. In this implementation, the MPC also treats the throttle control as part of the plant. These interactions are shown in Fig. 2.

The MPC utilises selected engine state measurements and estimations, as well as an engine speed and torque preview $\mathcal{V} = [\mathbf{v}_j, \mathbf{v}_{j+1}, \dots, \mathbf{v}_{j+N_p}]^T$, to determine a control trajectory $\mathcal{U} = [\mathbf{u}_j, \mathbf{u}_{j+1}, \dots, \mathbf{u}_{j+N_p-1}]^T$, where N_p is the number of sub-intervals of t_s second duration in the prediction horizon.

For this LTV-MPC, the inequality constraints

$$\mathbf{H}(\mathbf{x}_j, \mathbf{v}_j, \mathbf{u}_{j-1}) \geq \mathbf{0}, \quad (10)$$

are comprised of hard constraints on the available actuators (ζ_i , ζ_e and W_{LP-EGR}), as well as a soft constraint on the intake manifold concentration, defined as a conditional function

$$\xi_{i,max}(t_k) \leq \begin{cases} \xi_{b,max}^* + \epsilon_k & BMEP(t_k) \geq BMEP_{thr} \\ \xi_{i,thr} + \epsilon_k & BMEP(t_k) < BMEP_{thr} \end{cases}, \quad (11)$$

where $\xi_{b,max}^*$ is the target high load EGR rate, and the subscript k denotes the prediction horizon stage. The soft constraint is implemented with a relaxation factor ϵ_k in order to tolerate noise and modelling errors that may lead to the LTV-MPC problem being infeasible. In this paper, a representative set of threshold conditions are chosen, where $\xi_i < \xi_{i,thr} = 0.10$ at $BMEP_{thr} < 9$ bar.

The LTV-MPC cost function \mathcal{J} is the sum of the squares of the deviations of the stage outputs $\mathbf{y}_k = [\xi_{b,k}, \zeta_{i,k}, \zeta_{e,k}, \epsilon_k]^T$ from their corresponding reference values $\mathbf{y}_{ref,k} = [\xi_{b,k}^*, \zeta_{i,k}^{prod}, \zeta_{e,k}^{prod}, 0]$. The reference burned gas concentration pre-throttle ξ_b^* represents the rate of LP-EGR. This reference is defined as a conditional function

$$\xi_b^*(t_k) = \begin{cases} \xi_{b,max}^* & BMEP(t_k) \geq BMEP_{thr} \\ 0 & BMEP(t_k) < BMEP_{thr} \end{cases}. \quad (12)$$

As noted, previous research has suggested that high valve overlap at high load operation [13] may improve EGR evacuation rates. However, operation with modified valve timing may adversely affect engine breathing, or in the case of short-circuit flow through a stoichiometric DI engine, introduce periods of rich combustion. Therefore a cost is applied to deviation in valve timing from the baseline valve timings ζ_i^{base} , ζ_e^{base} , which are assumed to be well tuned for this engine. Finally, \mathcal{J} can incorporate a cost on the rate of change in \mathbf{u} , as needed, to suppress excessive input changes.

Given the linearised model (9) for a predictive component, the constraint set (10), and this cost function structure, the proposed LTV-MPC control law for a plant satisfying Assumptions 1-4 is

$$\mathbf{u} = \vartheta(\mathbf{x}_j, \mathbf{u}_{j-1}, \mathcal{V}), \quad (13)$$

where $\vartheta(\mathbf{x}_j, \mathbf{u}_{j-1}, \mathcal{V})$ corresponds to the first element \mathbf{u}_j of the control trajectory \mathcal{U} , and \mathcal{U} is obtained via solution of the optimal control problem:

$$\begin{aligned} \underset{\mathcal{U}}{\operatorname{argmin}} \mathcal{J} = & \sum_{k=j+1}^{j+N_p} (\mathbf{y}_k - \mathbf{y}_{ref,k})^T \mathbf{Q} (\mathbf{y}_k - \mathbf{y}_{ref,k}) \\ & + \sum_{k=j}^{j+N_p-1} (\mathbf{u}_k - \mathbf{u}_{k-1})^T \mathbf{R} (\mathbf{u}_k - \mathbf{u}_{k-1}), \end{aligned} \quad (14)$$

subject to: Equations (9),(10)

IV. MPC - CALIBRATION

A. Penalty on Deviation from Baseline Valve Timing

The components q , r of the diagonal weight matrices

$$\mathbf{Q} = \begin{bmatrix} q_1 & 0 & 0 & 0 \\ 0 & q_2 & 0 & 0 \\ 0 & 0 & q_3 & 0 \\ 0 & 0 & 0 & q_4 \end{bmatrix}, \quad \mathbf{R} = \begin{bmatrix} r_1 & 0 & 0 \\ 0 & r_2 & 0 \\ 0 & 0 & r_3 \end{bmatrix}$$

are chosen relative to the cost of a 1% point tracking error, $\xi_b - \xi_b^* = 0.01$. The cost of having ζ_i, ζ_e deviate from their baseline tuning is selected such that

$$q_1 \times 0.01^2 = q_2 (\zeta_{i,max} - \zeta_{i,min})^2 + q_3 (\zeta_{e,max} - \zeta_{e,min})^2,$$

so that deviating from baseline timing is undesirable except when necessary to meet the evacuation constraint during a tip-out. Note that in this paper, $q_2 = q_3$ and $r_1 = r_2$.

B. Soft Constraint Penalty

The final component of the \mathbf{Q} matrix is the weighting applied to the soft constraint violation ϵ_k . Ideally, ϵ_k is only non-zero when no feasible solution can be achieved otherwise, therefore, the associated cost q_4 is selected such that

$$\begin{aligned} q_4 \times 0.01^2 \gg & \sum_{k=j+1}^{j+N_p} (\mathbf{y}'_k - \mathbf{y}'_{ref,k})^T \mathbf{Q}' (\mathbf{y}'_k - \mathbf{y}'_{ref,k}) \\ & + \sum_{k=j}^{j+N_p-1} (\mathbf{u}_k - \mathbf{u}_{k-1})^T \mathbf{R} (\mathbf{u}_k - \mathbf{u}_{k-1}), \end{aligned}$$

where

$$\mathbf{y}'_k = [\xi_b, \zeta_i, \zeta_e], \quad \mathbf{Q}' = \begin{bmatrix} q_1 & 0 & 0 \\ 0 & q_{2,3} & 0 \\ 0 & 0 & q_{2,3} \end{bmatrix}.$$

Note that unlike the other cost function weights, q_4 is a function of N_p .

C. Actuator Rate Penalty

Selection of the weighting matrix \mathbf{R} requires additional manual tuning effort. As for \mathbf{Q} , the components of \mathbf{R} are chosen to penalise moving the full range of the actuators in a single sample interval, relative to $\xi_b - \xi_b^* = 0.01$. Tuning of \mathbf{R} is conducted using a representative engine cycle, with a desired pre-throttle EGR concentration $\xi_b^* = 0.25$, MPC sample interval $t_s = 0.05$ s, prediction horizon $t_p = 0.8$ s.

For this configuration, the components of \mathbf{R} are chosen such that the actuator penalties were one order of magnitude greater than a 1% point tracking error. This resulted in the anticipated valve overlap behaviour, and satisfaction of the ξ_i constraint.

Selecting smaller components for \mathbf{R} resulted in actuator chatter, and subsequent violation of the ξ_i constraint during the tip-out, whereas increasing \mathbf{R} offered diminishing improvements in suppressing actuator oscillation, and degraded tracking performance.

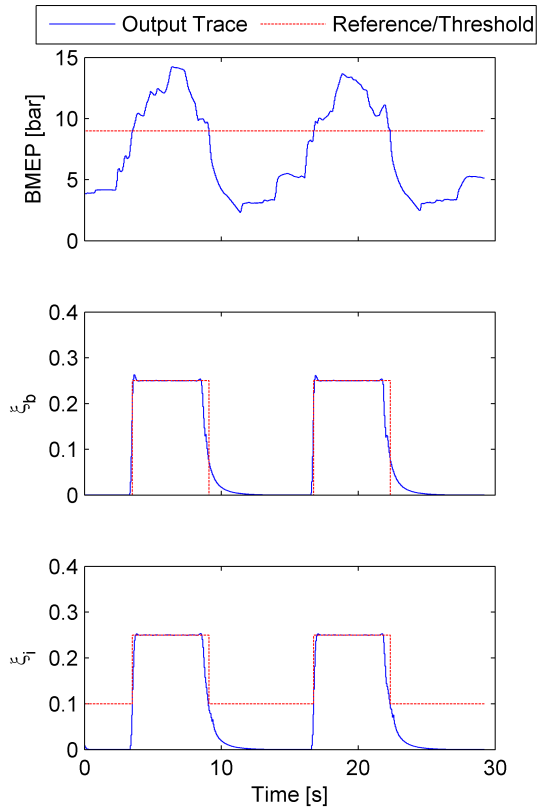


Figure 4. Control Simulation - $BMEP$ and States

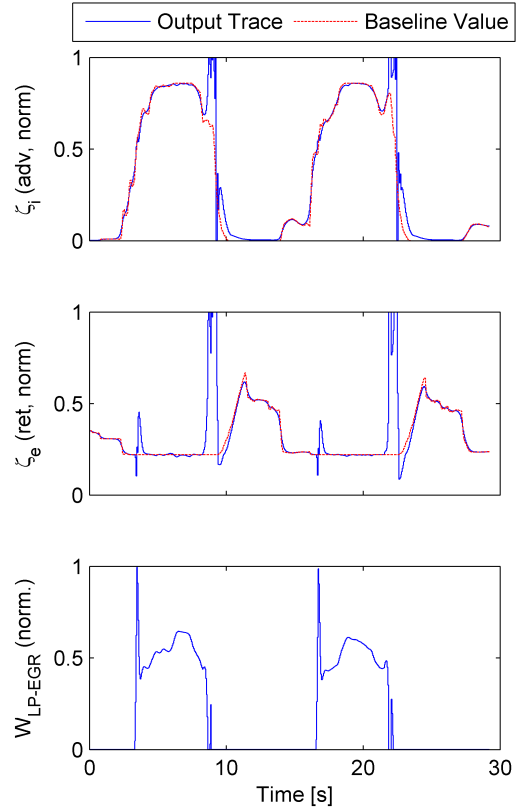


Figure 5. Control Simulation - Control Inputs

D. Simulation Results

Given a tuned set of \mathbf{R} values, the controller is applied to the representative, constant-engine-speed $BMEP$ transient plotted in Figure 4, and the results are shown in Figures 4 and 5. The ξ_i trace in Figure 4 demonstrates constraint satisfaction. The fact that the constraints are satisfied, combined with the high overlap ζ_i and ζ_e traces around the 9 and 22 second marks of Figure 5, indicate the use of scavenging as part of the optimised EGR evacuation process.

V. PREVIEW REQUIREMENTS FOR EGR EVACUATION

The preceding section established the potential for an MPC approach to achieve higher levels of EGR while still satisfying the state constraints. The MPC uses a priori knowledge of the torque trajectory to achieve this. As the required torque trajectory and the linearised plant model, may become less reliable the longer the preview period is, it is desirable to minimise the preview requirement for a given level of EGR above the threshold value $\xi_{i,thr}$. In this section, the minimum torque preview requirement is quantified in simulation for two cases: one with baseline valve timing, and another employing high valve overlap.

The two sets of controller simulations are run using the representative torque transient. In the first set, the constraints $\mathbf{H}(\mathbf{x}_j, \mathbf{v}_j, \mathbf{u}_{j-1})$ are modified so that ζ_i, ζ_e are limited to their baseline values. In the second set, the constraints are the limits

of actuation, as per the previous sections. In all cases, the prediction horizon and the torque preview period are assumed to be same. Both sets use the \mathbf{Q} , \mathbf{R} , and t_s values from the previous configurations.

To determine the minimum torque preview requirement, a series of simulations are conducted where N_p (and therefore, the torque preview) are varied, but are always shorter than the minimum physically needed for EGR evacuation. In each simulation, the maximum constraint violation is recorded, and these results are extrapolated to estimate the minimum required torque preview period. Note that when the preview period is shorter than required, \mathbf{Q} and \mathbf{R} no longer influence the result, as the weight applied to the constraint relaxation ϵ_k is much larger than all other weights.

This process is repeated for three levels of ξ_i^* , and the results are compiled in Fig. 6. The maximum amount of LP-EGR considered in this study is 25%, which is shown to require 0.48 s of preview (8 engine cycles at 2000 rpm) to satisfy the constraint without valve movement. Allowing deviations from the baseline VVT timing shortened the preview requirement by 0.06 s, or one engine cycle. Lower levels of EGR required shorter preview periods, but also reduced the benefit of high valve overlap. In fact, for 15% peak LP-EGR, the controller with valve overlap actually resulted in slightly slower evacuation rates.

These results suggest that the previously reported benefits of

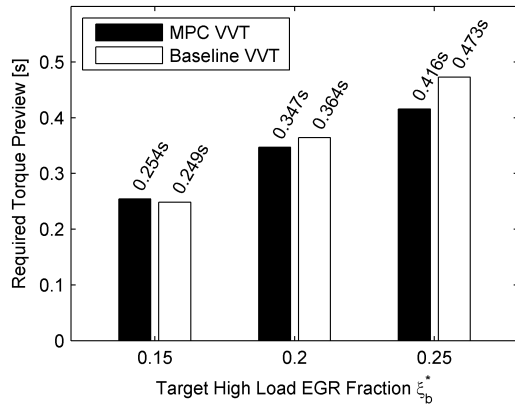


Figure 6. Torque Preview Requirements for EGR Evacuation

high valve overlap for evacuation, [13], are strongly contingent on maintaining the boosted condition that exists prior to tip-out. During the tip-out, the potential for short-circuit flow across the cylinder decreases with decreasing intake manifold pressure. This is particularly evident when comparing the 25% LP-EGR target with the 15% LP-EGR target. At 25%, the initial intake manifold pressure is higher, and short-circuit flow window is longer than at 15%, where the initial intake pressure prior to tip-out is lower.

Given the already idealised nature of this controller (see Assumption 4), it is likely that VVT deviations will not merit the additional controller complexity required for implementation.

VI. CONCLUSIONS

This paper presented development and simulation of a Linear, Time-Varying Model Predictive Control for the LP-EGR system of a GTDI engine. The internal predictive model was obtained through successive linearisation of a 2-state nonlinear model of the burned gas concentration in the intake manifold, and upstream of the throttle.

The stated goal of the controller was to increase the peak LP-EGR rates at low-speed, high-load engine conditions by managing EGR evacuation during tip-out; thereby addressing the limiting constraint, the maximum intake manifold burned gas concentration at lower loads. In the first instance, the LTV-MPC the cost function weights were tuned in simulation for a 0.8 s prediction horizon. This prediction horizon was chosen based on the accuracy of the linearised model.

The tuned controller was employed, in simulation, to determine preview period requirements for constraint satisfaction at 15%, 20% and 25% peak LP-EGR concentrations. For a fixed engine speed and a representative transient torque demand, the preview period required was shown to be 0.48 s for a peak LP-EGR rate of 25%.

Finally, the LTV-MPC was given authority over the valve timing, in order to evaluate the effectiveness of scavenging as a tool for reducing LP-EGR evacuation times. Simulation results indicated that scavenging reduced the LP-EGR evacuation by 0.06s, or one engine cycle for the 25% peak LP-EGR

case. However, the improvement was smaller for the 15% and 20% EGR cases, as the initial pressure differential became less favourable for scavenging. Given that the controller was tested assuming several idealisations, the small benefit due to scavenging will likely not merit further development of this approach.

ACKNOWLEDGMENTS

The authors gratefully acknowledge Yash A. Imai of Ford Motor Company for providing the GT-Power model on which the engine flow and concentration models were based, and Mrdjan Jankovic also of Ford Motor Company for valuable discussions that contributed to this work.

REFERENCES

- [1] A. Cairns, N. Fraser, and H. Blaxill. Pre versus post compressor supply of cooled EGR for full load fuel economy in turbocharged gasoline engines. In *SAE Technical Paper*, number 2008-01-0425, 2008.
- [2] S. Di Cairano, D. Yanakiev, A. Bemporad, I. V. Kolmanovskiy, and D. Hrovat. Model predictive idle speed control: Design, analysis and experimental evaluation. *IEEE Transactions on Control Systems Technology*, 20(1):84–97, January 2012.
- [3] O. Flardh, G. Ericsson, E. Klingborg, and J. Martensson. Optimal air path control during load transients on a spark ignited engine with variable geometry turbine and variable valve timing. *IEEE Transactions on Control Systems Technology*, 22(1):83–93, January 2014.
- [4] L. Guzzella and C. H. Onder. *Introduction to Modeling and Control of Internal Combustion Engine Systems*. Springer-Verlag Berlin Heidelberg, 2nd edition, 2010.
- [5] B. Haber and J. Wang. Robust control approach on diesel engines with dual-loop exhaust gas recirculation systems. In *Proceedings of the ASME 2010 Dynamic Systems and Control Conference DSCC2010*, 2010.
- [6] A. Y. Karnik, M. J. Jankovic, and M. H. Shelby. Scavenging in a turbocharged gasoline engine. *Int. J. Powertrains*, 1(4):420–437, 2012.
- [7] P. Langthaler and L. del Re. Robust model predictive control of a diesel engine airpath. In *Proceedings of the 17th IFAC World Congress*, 2008.
- [8] D. B. Roth, P. Keller, and M. Becker. Requirements of external EGR systems for dual cam phaser turbo GDI engines. In *SAE Technical Paper*, number 2010-01-0588, 2010.
- [9] M. Santillo and A. Karnik. Model predictive control design for throttle and wastegate control of a turbocharged engine. In *2013 American Control Conference*, pages 2183–2188. IEEE, 2013.
- [10] R. Sharma, D. Nestic, and C. Manzie. Idle speed control using linear time varying model predictive control and discrete time approximations. In *2010 IEEE International Conference on Control Applications*, 2010.
- [11] D. Takaki, H. Tsuchida, T. Kobara, M. Akagi, T. Tsuyuki, and M. Nagamine. Study of an EGR system for downsizing turbocharged gasoline engine to improve fuel economy. In *SAE Technical Paper*, number 2014-01-1999, 2014.
- [12] H. Wei, T. Zhu, G. Shu, L. Tan, and Y. Wang. Gasoline engine exhaust gas recirculation - a review. *Applied Energy*, 99:534–544, 2012.
- [13] A. P. Wiese, A. G. Stefanopoulou, A. Y. Karnik, and J. H. Buckland. Modelling and control of engine torque for short-circuit flow and egr evacuation. In *SAE World Congress*, number 17PFL-0751/2017-01-0606, 2017.
- [14] F. Yan and J. Wang. Control of diesel engine dual-loop EGR air-path systems by a singular perturbation method. *Control Engineering Practice*, 21:981–988, 2013.
- [15] Le Sollic G. Youssef, B., G. Corde, O. Hayat, C. Jabeur, and P. Olivier Calendini. Low pressure EGR control for a turbocharged diesel HCCI engine. In *18th IEEE International Conference on Control Applications*, 2009.